Optics Letters

Broadband electric-field-induced LP_{01} and LP_{02} second harmonic generation in Xe-filled hollow-core PCF

Jean-Michel Ménard,[1,2,3,*] Felix Köttig,[1,2] and Philip St.J. Russell[1,2]

[1]Max Planck Institute for the Science of Light, Erlangen, Germany
[2]Max Planck Centre for Extreme and Quantum Photonics, University of Ottawa, Ottawa, Ontario, Canada
[3]Department of Physics, University of Ottawa, Ottawa, Ontario, Canada
*Corresponding author: jean-michel.menard@uottawa.ca

Received 24 May 2016; revised 11 July 2016; accepted 20 July 2016; posted 20 July 2016 (Doc. ID 266915); published 5 August 2016

Second harmonic (SH) generation with 300 fs pump pulses is reported in a xenon-filled hollow-core photonic crystal fiber (PCF) across which an external bias voltage is applied. Phase-matched intermodal conversion from a pump light in the LP_{01} mode to SH light in the LP_{02} mode is achieved at a particular gas pressure. Using periodic electrodes, quasi-phase-matched SH generation into the low-loss LP_{01} mode is achieved at a different pressure. The low linear dispersion of the gas enables phase-matching over a broad spectral window, resulting in a measured bandwidth of ~10 nm at high pump energies. A conversion efficiency of ~18%/mJ is obtained. Gas-filled anti-resonant-reflecting hollow-core PCF uniquely offers pressure-tunable phase-matching, ultra-broadband guidance, and a very high optical damage threshold, which hold great promise for efficient three-wave mixing, especially in difficult-to-access regions of the electromagnetic spectrum.

OCIS codes: (060.5295) Photonic crystal fibers; (190.4223) Nonlinear wave mixing; (230.7405) Wavelength conversion devices.

http://dx.doi.org/10.1364/OL.41.003795

Second-order nonlinear crystals are commonly used for parametric frequency conversion at optical frequencies. Some of the most common applications are the generation of optical second harmonic (SH), three-wave mixing amplification, creation of entangled photon pairs, and generation of phase-locked terahertz transients. These noncentrosymmetric crystals have a high nonlinear $\chi^{(2)}$ coefficient, which is required for efficient three-wave mixing. Other important parameters are the spectral transmission window (which must span all the required frequencies), the linear dispersion (for phase-matched interactions with minimum group velocity walk-off of short pulses), and a high optical damage threshold. Gas-filled kagomé-style hollow-core photonic crystal fiber (HC-PCF) uniquely offers an optical platform with precise pressure-controllable linear dispersion [1]. Guiding by anti-resonant-reflection, kagomé-PCF features low-loss broadband guidance which, combined with its ability to maintain high intensities over long distances, makes it ideal for exploring extreme third-order nonlinear optical effects in traditionally hard-to-access regions of the electromagnetic spectrum, such as the ultraviolet (UV) and the mid-infrared [1–4]. Second-order nonlinear processes do not, however, occur under normal circumstances in HC-PCF, since both gas and glass are amorphous, i.e., centrosymmetric on average, with vanishingly small $\chi^{(2)}$.

In a previous experiment using narrow-linewidth nanosecond (ns) optical pump pulses, a second-order nonlinearity was created in HC-PCF by applying a high dc electric field E_{dc} across the fiber core [5]. This breaks the centrosymmetry and induces an effective $\chi^{(2)} \propto \chi^{(3)} E_{dc}$. Here we extend this idea to femtosecond (fs) pump pulses and report a SH conversion efficiency that is more than three orders of magnitude higher than previously achieved with ns pulses [5]. Moreover, we demonstrate that the use of periodic electrodes and pressure-tuning allows quasi-phase-matched SH generation directly into the low-loss LP_{01} mode.

The experimental configuration is sketched in Fig. 1(a). The optical pump source is an ytterbium-doped fiber laser generating 300 fs pulses at $\lambda = 1030$ nm at a repetition rate of 151 kHz. The pulses were launched into the LP_{01} mode of a 32-cm-long Xe-filled hollow-core kagomé-PCF, which was placed between a pair of 16-cm-long electrodes (although small fractions of higher-order modes can be excited, these are far from phase-matched for SH generation). Two 8-cm-long pigtails were extended outside the region under electrical bias, allowing both fiber ends to be placed inside gas cells. The kagomé-PCF was selected on the basis of its guiding properties, which featured relatively low propagation loss for the LP_{01} mode ($<2 \pm 0.5$ dB/m, measured using cutback) over a broad spectral region that included the pump frequency and its SH. A square-wave-modulated voltage (frequency 10 Hz) was applied to the electrodes, with zero average voltage, so as to prevent space-charge accumulation. When uniform electrodes were used [i.e., not periodically patterned as in Fig. 1(a)], a SH signal was detected in the LP_{02} mode at the phase-matching pressure of

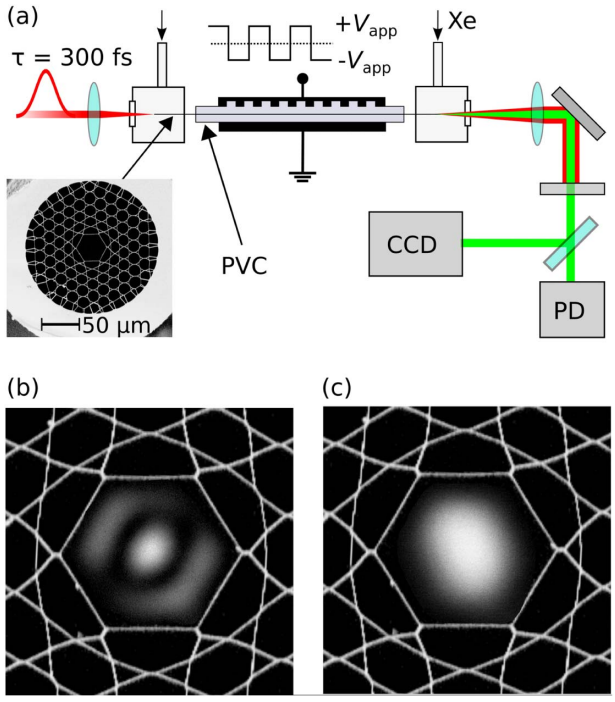

Fig. 1. Schematic of the experimental configuration. The ultrafast laser delivers pulses centered at $\lambda = 1030$ nm with a duration of $\tau = 300$ fs. A square-wave-modulated voltage (maximum amplitude $V_{app} = \pm 6.6$ kV and frequency 10 Hz) is applied across the Xe-filled kagomé-PCF. To avoid electrical breakdown in air, 100-μm-thick PVC sheets were inserted between the electrodes and the PCF. A silicon (Si) photodiode (PD) and CCD camera were used to characterize the SH. Inset: scanning electron micrograph (SEM) of the kagomé-PCF: the flat-to-flat core diameter is 33.2 μm. (b) and (c) Measured near-field intensity distributions (linear scale) of the SH signal (b) in the LP_{02} mode when intermodal phase-matching conditions are satisfied and (c) in the LP_{01} mode when a periodic electrode allows QPM. An SEM of the fiber core structure is superimposed on the images for reference.

$P_{Xe} = 3.86$ bar. A theoretical model based on a modified capillary waveguide [6] indicates that intermodal phase-matching conditions are satisfied at this pressure, using the tabulated refractive index of xenon [7] as well as the PCF parameters: a flat-to-flat core diameter of 33.2 μm, a core wall thickness of 190 nm, and an empirical s-parameter [6] of 0.09.

In a second experiment, a SH signal was generated directly in the LP_{01} mode by quasi-phase-matching (QPM) using periodic electrodes formed from copper strips with a mark-space ratio of 1. The relatively low dispersion of kagomé-PCF means that the required QPM period Λ could be as long as 2 mm. As a result, standard printed circuit board techniques could be used to fabricate the electrodes. The pressure P_{Xe} was then adjusted until a SH signal was observed in the LP_{01} mode.

To prevent electrical discharge in air, polyvinyl chloride (PVC) film sheets (100 μm thick) were inserted between the PCF and each electrode. A nonconductive glue was used to hermetically seal the section of the fiber under electrical bias. This allowed us to apply a maximum voltage $V_{app} = 6.6$ kV to the electrodes without breakdown. Considering the diameter of the air-like photonic crystal cladding (170 μm), the thickness of the encircling silica sheath (47 μm), and the dielectric constants of silica (3.8) and PVC (3.2), we estimated the maximum field amplitude in the fiber core to be $E_{dc} = 260$ kV/cm. The SH power was measured with a Si photodiode after filtering out the residual pump light. The mode profile was observed by imaging the end-face of the fiber with a CCD camera. Finally, the spectrum of the SH signal was monitored using an optical spectrum analyzer [not shown in Fig. 1(a)].

The intermodal SH signal, generated in the LP_{02} mode [Fig. 1(b)], was first investigated as a function of the launched pump pulse energy W_P. As shown in Fig. 2(a), it increases quadratically as a function of the pump energy up to $W_P \sim 1$ μJ, in agreement with the theoretical model for electrically field-induced second harmonic generation (EFISH) in HC-PCF in the quasi-monochromatic and no-pump-depletion approximation [5]. Even though the ultrashort pulses in the experiment were highly nonmonochromatic [full width at half-maximum (FWHM) bandwidth 7 nm], they were efficiently converted into the SH. This is because of the relatively broad phase-matching band (11 nm FWHM for a 16-cm nonlinear interaction length between the pump and SH), made possible by the low linear dispersion of the system [6,7]. As W_P increased above 1 μJ, the SH signal gradually falls below its initial quadratic dependence on W_P. This is caused by the effects of self-phase modulation (SPM), which broadens and restructures the pump spectrum so that an increasingly large fraction of the pump spectrum lies outside the phase-matching band. A maximum SH pulse energy of $W_{SH} = 430$ pJ was measured at $W_P = 2$ μJ (peak intensity $\sim 3 \times 10^{12}$ W/cm^2), which was the highest pump energy we could use before thermal effects disturbed the fiber in-coupling alignment. This value of W_{SH} corresponds to a conversion efficiency of $\eta \sim 0.02\%$, which is ~2000 times higher than the maximum η previously reported in a similar EFISH experiment in HC-PCF using ns pump pulses [5]. Also, the normalized

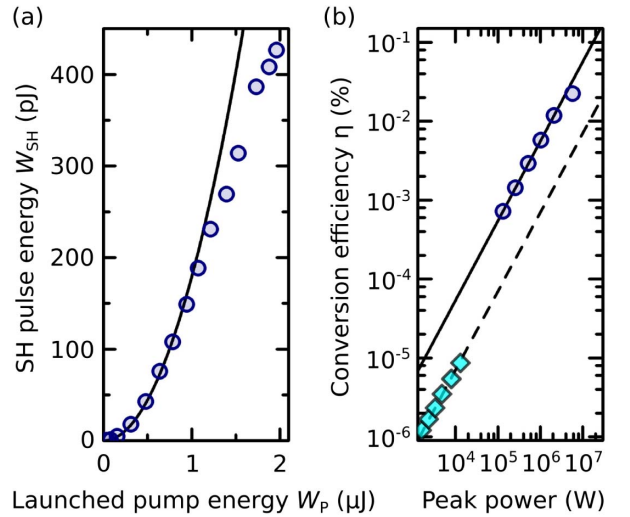

Fig. 2. (a) Pulse energy of the SH (W_{SH}) in the LP_{02} mode as we vary the pump pulse energy W_P. The gas pressure P_{Xe} is optimized to yield the maximum SH signal. The applied dc field is $E_{dc} = 260$ kV/cm inside the fiber core. (b) Comparison between the SH conversion efficiencies η achieved in this work (blue circles) and previous electrically field-induced second harmonic generation (EFISH) experiments in Xe-filled hollow-core PCF using 2-ns pump pulses (cyan diamonds) [5].

efficiency $\hat{\eta}$ in %/mJ corresponded to $\hat{\eta} = 18\%/\text{mJ}$ for $W_P < 1$ μJ and decreased to 10%/mJ at $W_P = 2$ μJ. This leveling off in efficiency at higher pump energies is caused by SPM broadening in the pump. In comparison, $\hat{\eta} = 0.00034\%/\text{mJ}$ for the data reported in [5].

Figure 2(b) compares η extracted from selected data-points in [5] and Fig. 2(a) as a function of the optical peak power, making possible a direct comparison between the SH signal generated by ns and fs pump pulses. The dramatic increase in η reported in this Letter can be attributed to two factors, both related to the new experimental configuration. First, the ultrafast pump laser in the current experiment delivered higher peak powers, resulting in a 200-fold increase in η. Second, a more robust electrode design allowed higher values of E_{dc}, resulting in larger values of $\chi^{(2)}$ and increasing η by about another order of magnitude [Fig. 2(b)]. Electrical breakdown, which resulted in a sudden drop in electric field across the core, limited the maximum applied electric field to ~260 kV/cm. Breakdown occurred in sub-mm-wide regions randomly located along the electrodes and was probably caused by localized defects in the PVC sheets. Improved designs, such as one involving microelectrodes built directly inside the PCF [8], would allow higher efficiencies of SH generation.

The maximum SH signal in the LP_{02} mode occurred consistently at $P_{Xe} = 3.86$ bar for low pump energies $W_P < 0.5$ μJ. This agrees with the predictions of intermodal phase-matching [6]. For higher values of W_P, however, the SH signal was strongest at lower pressures (Fig. 3) and shifted toward the blue (Fig. 4). For instance, at $W_P = 2$ μJ, which was the highest pump energy used in the experiment, the SH signal was maximum at $P_{Xe} = 3.79$ bar and ~25% lower at $P_{Xe} = 3.86$ bar [note that each data-point in Fig. 2(a) was collected after optimizing the SH output power]. We attribute this behavior to the complex interplay of SPM-induced spectral broadening in the pump pulse, pressure-dependent phase-matching conditions, and group velocity walk-off (GVW) between pump and SH. The SH signal was measured as a function of W_P at a constant pressure of 3.83 bar (Fig. 4); at this pressure, theory predicts that the SH signal will be strongest at $\lambda = 514$ nm. At $W_P = 0.5$ μJ, the SH spectrum has a Gaussian-like distribution centered at 515 nm with a FWHM of ~3 nm. As W_P increases, the spectrum gradually broadens, reaching a FWHM maximum of ~10 nm at

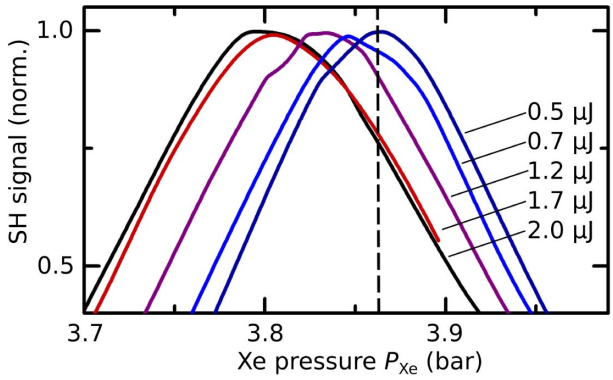

Fig. 3. SH signal as a function of xenon pressure P_{Xe} at various pump energies W_P. For $W_P \leq 0.5$ μJ, the maximum SH signal was consistently observed at $P_{Xe} = 3.86$ bar (vertical dashed line).

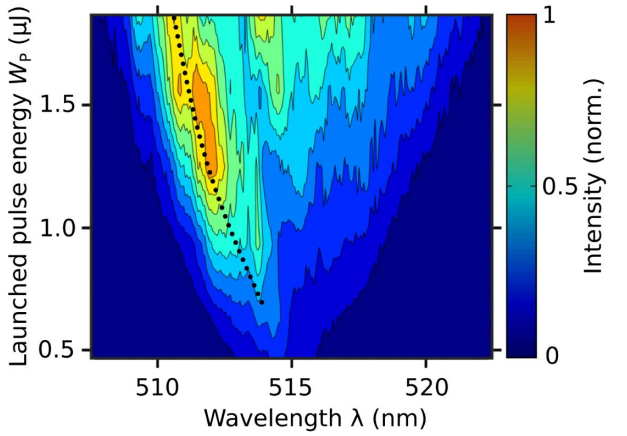

Fig. 4. Spectrum of the EFISH signal as a function of W_P. The dotted line follows the main feature: a peak that gradually shifts from 514 to 511 nm as W_P increases from 0.7 to 2 μJ.

$W_P = 2$ μJ. Besides these broadening effects, the output SH spectrum also becomes increasingly structured, its most prominent feature being a peak (dotted line in Fig. 4) that shifts from 514 to 511 nm as W_P is increased from 0.7 μJ to 2 μJ. We attribute this structuring to SPM-related broadening effects in the pump pulse. The broad linewidth of the SH signal confirms that gas-filled kagomé-PCF is suitable for efficient frequency conversion of ultrashort pulses. In a 16-cm-long electrically biased Xe-filled HC-PCF, SH can be generated over a 10-nm bandwidth at $\lambda \sim 515$ nm, which corresponds to the FWHM spectral linewidth of a ~100 fs transform-limited pulse. Furthermore, the electrode length can easily be shortened or lengthened so as to adjust the nonlinear phase-matching bandwidth.

In a second experiment, periodic QPM electrodes were used to generate a SH signal directly in the low-loss LP_{01} mode. As usual in QPM, the phase-matching period is given by $\Lambda = \lambda_{SH}/(|n_{SH} - n_P|$, where λ_{SH} is the SH wavelength, n_{SH} the modal index at the SH, and n_P the pump mode index. A low pump energy (0.24 μJ) was used to prevent spectral broadening. Also, to maximize the on-off contrast of the periodic E_{dc} inside the PCF core, the QPM electrode was placed in direct contact with the PCF by removing the upper PVC sheet in Fig. 1(a). UV glue was not used in this case, permitting ten different QPM electrodes, with pitches Λ ranging from 1.2 to 1.9 mm, to be used. Removal of the PVC sheet meant, however, that electrical breakdown occurred at a lower voltage, limiting the in-core electric field to ~40 kV/cm. With our current QPM geometry, $\eta \sim 0.0001\%$ was achieved when $\Lambda = 1.2$ mm. Optimum SH conversion efficiency would require careful design of the periodic electrode system to avoid breakdown—a topic for future research.

Upon applying a voltage across the electrodes and scanning P_{Xe}, two prominent SH peaks were consistently recorded [Fig. 5(a)]. The first was at $P_{Xe} = 3.86$ bar, corresponding to the LP_{02} mode described in the first experiment; SH signals of similar strength (±20%) were observed in this mode for all the periodic electrodes used in the experiment. A second peak was seen at different pressures depending on the QPM period, for example, at $P_{Xe} = 4.1$ bar for $\Lambda = 1.82$ mm (dark blue

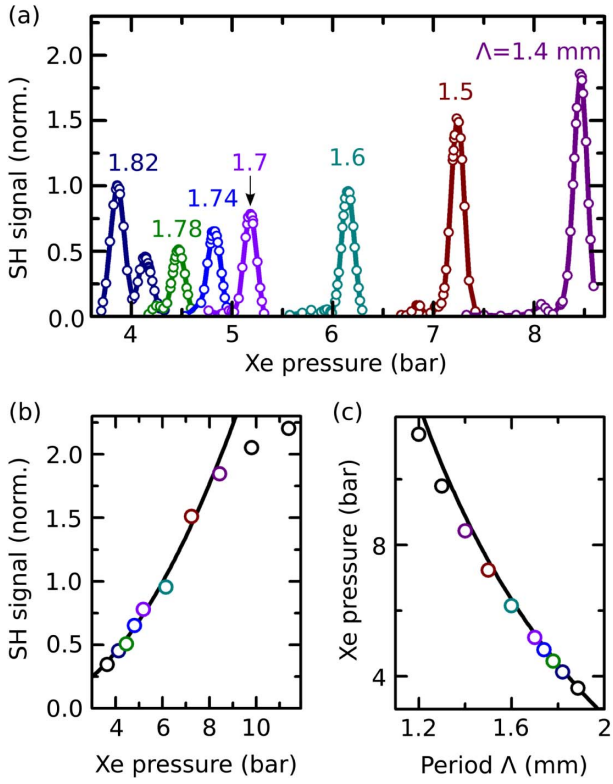

Fig. 5. (a) SH signals in the LP_{01} mode are generated at gas pressures P_{Xe} that vary with the period Λ of the QPM electrode. At 3.86 bar, the LP_{02} mode is observed for all Λ. Only the data corresponding to $\Lambda = 1.82$ mm are shown (dark blue curve) for clarity. (b) The SH signal (circles) in the LP_{01} mode follows a quadratic dependence on P_{Xe} (black curve) up to ~8 bar, at which point the signal starts to saturate due to group velocity walk-off. (c) Optimal P_{Xe} for QPM SH generation as a function of Λ. Experimental data (circles) agree well with analytical calculations (black curve) using the model in [6], assuming a flat-to-flat core diameter of 33.2 μm, a core wall thickness of 190 nm, and an s-parameter of 0.09. The refractive index of xenon was taken from [7].

curve). In every case this other SH signal was in the LP_{01} mode [see near-field optical micrograph in Fig. 1(c)].

Since $\chi^{(3)}$ scales linearly with the gas pressure [9], a stronger SH signal is generated for smaller QPM periods when the phase-matching pressure is higher. Figure 5(b) shows the dependence of the SH signal strength on P_{Xe} (circles). It is quadratic, as expected from a quasi-CW model [5] (black curve), but saturates for $P_{Xe} \geq 10$ bar as a result of GVW between pump and SH pulses. Calculations [6] show that GVW has an almost perfectly linear dependence on pressure between 4 bar (~0 fs/cm) and 10 bar (~11 fs/cm). Considering the 16-cm-long interaction length, the GVW at $P_{Xe} = 10$ bar is ~180 fs, which is more than half the pump pulse duration ($\tau = 300$ fs) and thus significantly reduces the effective nonlinear interaction length. Note that the QPM conversion efficiency could be enhanced by a factor of 4 if the electrodes were designed to produce an alternating electric field instead of the unipolar electrode used in the current experiment. The combination of the QPM period and the pressure at which phase-matching occurs [circles in Fig. 5(c)] is also well predicted by the analytical theory [6] [black line in Fig. 5(c)]. This confirms that the linear and nonlinear properties governing efficient three-wave mixing in electrically biased Xe-filled kagomé-PCF can be accurately estimated from the PCF structural parameters and the gas pressure alone.

In conclusion, effective second-order nonlinear conversion of femtosecond optical pulses can be achieved by applying an electrical bias across a Xe-filled hollow-core kagomé-PCF. The SH can be generated in the LP_{02} mode by intermodal phase-matching or intramodally in the LP_{01} mode if QPM is used. For 300 fs pump pulses, nonlinear conversion efficiencies as high as $\hat{\eta} = 18\%/\text{mJ}$ (or $\eta \sim 0.02\%$) could be obtained, with bandwidths of ~10 nm. Gas-filled kagomé-PCF (or any of the several anti-resonant reflecting PCF designs [1,10–12]) provides broadband low-loss transmission, pressure-tunable dispersion, and a high damage threshold. These features are ideal for achieving efficient three-wave mixing with ultrashort pulses in difficult-to-access regions of the electromagnetic spectrum, such as the ultraviolet or the terahertz. An important hurdle still to be cleared is the relatively low nonlinear coefficient $\chi^{(2)}$ reached in the electrical poled gas. Although QPM permits phase-matching to be achieved at higher pressures, thus increasing the effective value of $\chi^{(2)}$, the most promising solution is to increase the electrical field in the core. This could be accomplished, for example, by incorporating metallic electrodes in selected hollow channels in the cladding so as to reduce the effects of electrical breakdown. A new regime of nonlinear optics, in which the electrically biased plasma contributes to three-wave mixing processes as a distinct nonlinear medium, may then become accessible [13], providing interesting insights into the nonlinear optics of plasmas.

Acknowledgment. We thank O. Bittel and L. Meier for their technical assistance and for useful discussions.

REFERENCES

1. P. St.J. Russell, P. Hölzer, W. Chang, A. Abdolvand, and J. C. Travers, Nat. Photonics **8**, 278 (2014).
2. F. Belli, A. Abdolvand, W. Chang, J. C. Travers, and P. St.J. Russell, Optica **2**, 292 (2015).
3. N. Y. Joly, J. Nold, W. Chang, P. Hölzer, A. Nazarkin, G. K. L. Wong, F. Biancalana, and P. St.J. Russell, Phys. Rev. Lett. **106**, 203901 (2011).
4. A. M. Jones, A. V. V. Nampoothiri, A. Ratanavis, T. Fiedler, N. V. Wheeler, F. Couny, R. Kadel, F. Benabid, B. R. Washburn, K. L. Corwin, and W. Rudolph, Opt. Express **19**, 2309 (2011).
5. J.-M. Ménard and P. St.J. Russell, Opt. Lett. **40**, 3679 (2015).
6. M. A. Finger, N. Y. Joly, T. Weiss, and P. St.J. Russell, Opt. Lett. **39**, 821 (2014).
7. A. Börzsönyi, Z. Heiner, M. P. Kalashnikov, A. P. Kovács, and K. Osvay, Appl. Opt. **47**, 4856 (2008).
8. H. W. Lee, M. A. Schmidt, H. K. Tyagi, L. P. Sempere, and P. St.J. Russell, Appl. Phys. Lett. **93**, 56 (2008).
9. D. P. Shelton, Phys. Rev. A **42**, 2578 (1990).
10. P. Uebel, M. C. Günendi, M. H. Frosz, G. Ahmed, N. N. Edavalath, J.-M. Ménard, and P. St.J. Russell, Opt. Lett. **41**, 1961 (2016).
11. F. Yu, W. J. Wadsworth, and J. C. Knight, Opt. Express **20**, 11153 (2012).
12. Y. Y. Wang, N. V. Wheeler, F. Couny, P. J. Roberts, and F. Benabid, Opt. Lett. **36**, 669 (2011).
13. P. Hölzer, W. Chang, J. C. Travers, A. Nazarkin, J. Nold, N. Y. Joly, M. F. Saleh, F. Biancalana, and P. St.J. Russell, Phys. Rev. Lett. **107**, 203901 (2011).